OPEN ACCESS
IOP Publishing
Journal of Physics B: Atomic, Molecular and Optical Physics
J. Phys. B: At. Mol. Opt. Phys. **48** (2015) 065201 (7pp)
doi:10.1088/0953-4075/48/6/065201

R-matrix with pseudostates study of single photon double ionization of endohedral Be and Mg atoms

T G Lee[1], C P Ballance[1], S A Abdel-Naby[1,2], J L King[1], T W Gorczyca[3] and M S Pindzola[1]

[1] Department of Physics, Auburn University, Auburn, AL 36849, USA
[2] Department of Physics, Beni Suef University, Beni Suef, Egypt
[3] Department of Physics, Western Michigan University, Kalamazoo, MI 49008, USA

E-mail: tgl0002@auburn.edu

Received 30 June 2014
Accepted for publication 21 January 2015
Published 20 February 2015

Abstract

We perform *R*-matrix with pseudostates calculations to investigate single photon double ionization of Be@C_{60} and Mg@C_{60}. We contrast the present results to our previous studies of He@C_{60}. We find the presence of the confinement resonances in the double photoionization cross sections of endohedral Be and Mg. Keeping the same C_{60} spherical shell potential in each case for these systems, we explore the change in magnitude and the energy dependence of the resonance features relative to the background cross sections.

Keywords: atomic collision, photoinization, molecular physics

(Some figures may appear in colour only in the online journal)

1. Introduction

Ejection of two electrons from atoms or molecules after single photon absorption is of fundamental interest as the process involves two continuum electrons moving in the long range Coulomb field of the resulting ion. Considerable experimental and theoretical investigations of this process have been carried out over the past 15 years. A number of atoms were studied, but special attention has always been dedicated to the proto-typical two-electron helium atom.

The double photoionization cross section of He has been theoretically determined with sufficient accuracy using a number of non-perturbative theoretical methods such as the hyperspherical close-coupling [1, 2], convergent close-coupling (CCC) [3], eigenchannel *R*-matrix (RM) [4, 5], *R*-matrix with pseudostates (RMPS) [6] and time-dependent close-coupling (TDCC) [7–10]. The theoretical results were found to be in very good agreement with the experimental measurements [11–13].

In recent years, photoionization of endofullerenes—atoms encapsulated inside a fullerene—has been a subject of theoretical and experimental interest. Unlike the 'free' atom, the additional cage interaction has proven to give rise to intriguing oscillatory structures in the photoionization cross section—a phenomenon known as confinement resonances. Theoretical studies have illustrated that this phenomenon arises from the multi-path wave-interference between photo-electrons emitteds from the encapsulated atom and photo-electrons reflected from the inner and outer boundaries of the fullerene cage. A review on the current status of the experimental and theoretical progress in the field of photo-induced ionization of endohedral atoms has been reported in [14].

Experimental measurement of confinement resonances, especially in double photoionization, is considerably challenging. This is because the single photon double ionization of an atom is a second-order process and the magnitude of its cross section can be typically several hundreds to thousands times smaller than the first-order single ionization process. In 2010 Kilcoyne *et al* [15] successfully measured the

confinement resonances associated with double photoionization of the Xe atom in the bucky-fullerene C_{60} cage. The experimental measurements were made at the advanced light source (ALS) in the photon energy range from 60 eV to 150 eV by merging a mass-selected $Xe@C_{60}^{+}$ ion beam with a beam of monochromatized synchrotron radiation. On the other hand, an earlier experiment by Müller and collaborators [16] of single and double photoionization of $Ce@C_{82}^{+}$ ion, however, indicated no evidence of oscillatory structures in the cross sections due to confinement resonances.

On the theoretical side, the presence of the confinement resonances in the double photoionization cross section of $He@C_{60}$ was predicted using an analytical model by Amusia *et al* [17], a few years before the ALS's experiment [15]. The presence of the confinement resonances in the double ionization cross section of $He@C_{60}$ was later confirmed using a non-perturbative TDCC method with a square-well potential, which effectively represents the spherical shell [18, 19].

An alternative and yet equally powerful non-perturbative RM method has also been extended to study the confinement resonances in photonionization cross section of atoms. Unlike the TDCC method, the RM method is more practical for treating long-lived atomic resonances and multi-electron atomic systems. For example, the standard RM method has been successfully employed to study the single photoionization of $Xe@C_{60}$ [20] and $Ca@C_{60}$ [21]. Similar to the TDCC approach, a well-established square-well potential has been adopted to model the fullerene cage. More recently, the same square-well potential has also been implemented in the advanced RMPS method to study the photoionization with excitation and double photoionization of benchmarked He and $He@C_{60}$ systems [22]. The RMPS results were found to be in excellent agreement with the TDCC calculations. In addition, the RMPS method has also been used to determine the total cross section for double photoionization of Be and Mg atoms. Again, the RMPS method gives a cross section in good agreement with those from the TDCC and the CCC methods. All together, the calculated cross sections agree well with the available experimental data [23].

In viewing of future experimental investigations on the fullerene encapsulating alkaline-Earth atoms, it is desirable to carry out a theoretical study on such systems. Besides, to the best of our knowledge, the study of double photoionization of $Be@C_{60}$ and $Mg@C_{60}$ has never been considered. In this study, we apply the RMPS method to examine the double photoionization of $Be@C_{60}$ and $Mg@C_{60}$. Keeping the same C_{60} spherical shell potential in each case, we explore the magnitude and energy dependence of the resonance features relative to the background cross sections. Furthermore, the photoionization process of these systems are expected to be clean since it has been shown by Browclawik and Eilmes that in $Be@C_{60}$ and $Mg@C_{60}$ there is no electron transfer from the metal atom to the cage [24].

We organized the rest of the paper as follows. In section 2, we outline the computational details as applied to the endohedral atoms. The computed cross sections for double photoionization of $Be@C_{60}$ and $Mg@C_{60}$ are presented in section 3. Finally, a brief summary is given in section 4. Unless otherwise mentioned we used atomic units throughout the paper and 1.0 b = 10^{-24} cm^2.

2. Theoretical calculations

To model the fullerene shell, as in our recent study [22], we assume the confining potential is zero everywhere except for the spherical shell formed by the partially delocalized valence electrons of the carbon atoms. That is

$$V_c(r) = \begin{cases} -U_0, & r_0 \leqslant r \leqslant r_1 \\ 0, & \text{otherwise} \end{cases}, \tag{1}$$

where the inner radius $r_0 = 5.75$ a.u., the outer radius $r_1 = 7.64$ a.u. and the well depth $U_0 = 0.302$ a.u.. The determination of these values originates from the pioneering work of Xu *et al* [25] and Dolmatov *et al* [26] and these parameters have been employed in our previous work. We also note that the sensitivity of the photoionization cross sections to equation (1) and a diffuse model potential has been investigated recently and negligible difference between the two cross section results have been reported [27]. On the other hand, we caution the use of the rigid model potential may be problematic at low photon energies since one can imagine that the slowly moving photoelectron in the final state of the double photoionization can interact with fullerene electrons and therefore change the fullerene structure. Incidentally, it has been shown by Browclawik and Eilmes that the enclosed Be and Mg valence electrons in the initial state do not interact with the C_{60} [24].

To calculate the photoionization cross section we employed the *LS*-coupling RMPS method. The method is an extension of the standard RM approach. Briefly, in the standard RM method, the time-independent close-coupling equations of photoionization are solved by diving configuration space into two regions. An inner region in which electron–electron correlation and exchange are important and an outer region in which the exchange is neglected. This method enables the inner region problem to be solved using bound state methods and the outer region by solving a set of close-coupled equations for each continuum electron energy. By matching these two solutions at the boundary of the inner and outer regions through the RM, collision strengths are extracted.

In the RMPS method, a set of the pseudo orbitals are used to represent the high-Rydberg and continuum target states. The pseudo orbitals are generated from a set of non-orthogonal Laguerre radial wavefunctions. These Laguerre orbitals are then orthogonalized to the spectrocopic orbitals and to each other. A detailed description of the method can be found in [22, 23]. Here we only outline the essence in regard to the atomic structure calculation. For the double photoionization calculations of Be, we first carried out the spectroscopic structure calculations using the AUTOSTRUCTURE program [28] to obtain the Thomas–Fermi–Dirac–Amaldi (TFDA) spectoscopic {1s, 2s, 2p, 3s, 3p, 3d} orbitals, which we then suppplemented with a large set of Laguerre pseudostates $\{\bar{n}l\}$ for

$4 \leqslant \bar{n} \leqslant 16$ and $l = \{s, p, d, f\}$ for Be^+. This choice of basis orbitals resulted a smaller RM boundary radius of $R_a = 46.0$ a.u. as opposed to 50.4 a.u. in the earlier study [23]. Mathematically, the radial extent of the RM could be chosen to be any desired value. But, here it was determined by the last and most diffused orbital in the close-coupling expansion. With a few tests, it turns out that this is adequate for the present RM calculations.

From the AUTOSTRUCTURE calculations, we obtained the energies of the first nine terms of Be^+ relative to the ground term essentially identical to the values given in table I in [23], which closely agreed; to an average of $1.0 \sim 2.5\%$; with the NIST atomic spectroscopic data [29]. This is also true for the $1s^24l$ terms, even though the $4l$ wavefunctions were generated using a linear combination of Laguerre orbitals. The calculated energy of the $1s^22s^2\ ^1S$ ground term of Be relative to the $1s^22s\ ^2S$ ground term of Be^+ is −9.3133 eV compared to the experimental values of −9.3187 eV [29].

A similar set of calculations was performed for the double photoionization of the Mg atom. Here, we generated the TFDA spectoscopic {1s, 2s, 2p, 3s, 3p, 3d, 4s, 4p, 4d, 4f} orbitals, which we then added a large set of Laguerre pseudostates $\{\bar{n}l\}$ for $5 \leqslant \bar{n} \leqslant 16$ and $l = \{s, p, d, f, g\}$ for Mg^+. This set of basis orbitals also gives rise to the same RM boundary radius of $R_a = 46$ a. u. as opposed to a slightly larger RM radius of 51.3 a.u. in the previous work for Mg atom [23]. Nonetheless, from the atomic structure calculations, we reproduced the eigenenergies of the first 13 terms of Mg^+ relative to the ground term given in table II in [23] up to four significant figures. These values agreed reasonably well; to an average of $2.0 \sim 4.0\%$; with the NIST atomic spectroscopic data [29]. We note that the calculated energy of the $2p^63s^2\ ^1S$ ground term of Mg relative to the $2p^63s\ ^2S$ ground term of Mg^+ is −7.5317 eV compared to the experimental values of −7.6432 eV [29]. It is important to note that, in the present model calculations for endohedral alkali-Earth atoms, the C_{60} model potential was not considered in the AUTOSTRUCTURE calculations. Instead, it was implemented in the stage I of the RMPS method.

Our newly developed TDCC method has also been employed to calculate the double and single photoionization cross sections of free Be and Mg atoms. The method is based on an implicit time propagator with core orthogonalization approach on a variable mesh [30] as opposed to the one employed in Griffin *et al* [23] which used an explicit time propagator with a core-pseudopotential on a uniform mesh.

Briefly, in the present TDCC calculations of photoionization of free Be atom, we considered a 648^2-point variable mesh with starting radial step-size of $\Delta r = 0.01$ a.u. that gives a maximum radial box size of $R = 111.5$ a.u.. For the atomic structure calculations, we diagonalized the one-electron Hamiltonian equation in this box to obtain a complete set of bound plus continuum radial orbitals needed to calculate the photoionization probabilities. The atomic core potential parameters are optimized in order to obtain the 2s and 2p orbitals binding energies of 18.2 eV and 14.2 eV, respectively, which are in good agreement with the Be^+ experimental values $E_{2s} = 18.2$ eV and $E_{2p} = 14.3$ eV of the NIST's database [29]. To obtain the desired correlated initial state wavefunctions for photoionization calculations, the TDCC equations are relaxed in imaginary time on the same radial mesh with 7 coupled channels. We employed implicit time propagator with time step-size $\Delta t = 0.025$ a.u.. At each time step, the initial state wavefunctions are orthogonalized to the 1s orbital. The correlated initial state wavefunctions were found to have an energy of −27.6 eV, in close agreement with the experimental double ionization potential energy of 27.5 eV for Be atom [29]. To calculate the photoionization probabilities and hence the cross sections, the TDCC equations were propagated in real time with $\Delta t = 0.01$ a.u. and 12 coupled channels over 10 radiation field periods.

For the case of Mg atom, we considered a 720^2-point variable mesh with starting a finer radial step-size of $\Delta r = 0.005$ a.u. that yields a maximum radial box size of $R = 105.9$ a.u.. Similarly, the one-electron Hamiltonian equation was diagonalized with the atomic core potential parameters fine tuned such that one obtained the 3s and 3p orbitals binding energies of 15.0 eV and 10.6 eV, respectively, which agree well with the experimental values $E_{3s} = 15.0$ eV and $E_{3p} = 10.6$ eV of the NIST's database [29]. Same relaxation procedure of the TDCC equations in imaginary time with $\Delta t = 0.025$ a.u. on the 720^2-point radial mesh with 7 coupled channels was carried out to obtain the correlated initial state wavefunctions. The time step-size was kept at $\Delta t = 0.025$ a.u. in the implicit time propagator method and the ground *s*-wave coupled channel wavefunction was orthogonalized to the 1s and 2s orbitals, whereas the first excited *p*-wave coupled channel wavefunction was orthogonalized to the 2p orbital. The correlated initial state wavefunctions were found to have an energy of −22.8 eV, in good agreement with the double ionization potential energy of 22.7 eV for Mg documented in NIST's database [29]. In order to obtain the photoionization probabilities, the propagation of TDCC equations was carried out in real time with $\Delta t = 0.01$ a.u. and 12 coupled channels over 10 radiation field periods.

3. Results

To establish the numerical confidence of our present RMPS calculations, we first compute and compare the cross section for double photoionization of free Be and Mg from the ground term in figure 1. The RMPS results obtained here are in the length gauge. In the previous study by Griffin *et al* [23] it is shown that the results obtained in the length and velocity gauges are indistinguishable for the Be atom and are significantly close for the Mg atom. Therefore, a velocity gauge calculation is not necessary for the present purpose. Furthermore, we have checked the accuracy of the present calculations, even though the present calculations were carried out with a slightly smaller RM basis set, the data are comparable, with a maximum difference of approximately 3%, to the earlier RMPS results of [23]. The second purpose of

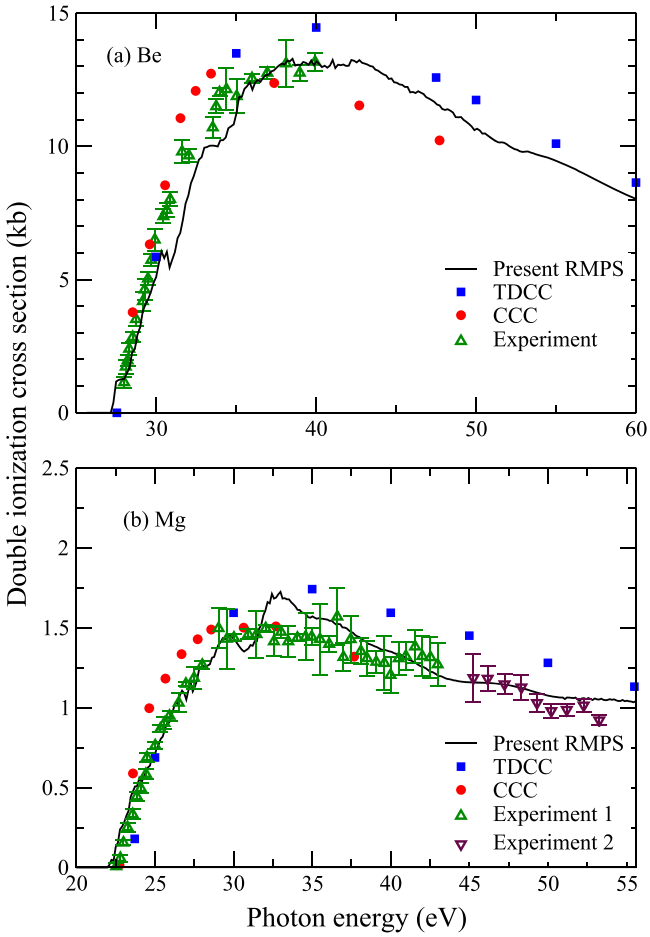

Figure 1. Double photoionization cross section of Be and Mg atoms as a function of photon energy. (a) Be atom: present TDCC results, CCC results from Kheifet and Bray [34], experiment: data from Wehlitz, Lukic and Bluett [35]. (b) Mg atom: present TDCC results, CCC results from Kheifets and Bray [36], experiment 1: data from Wehlitz, Juranic and Lukic [37]. Experiment 2: data inferred from the ratios of double to single photoionization from Wehlitz, Juranic and Lukic [37].

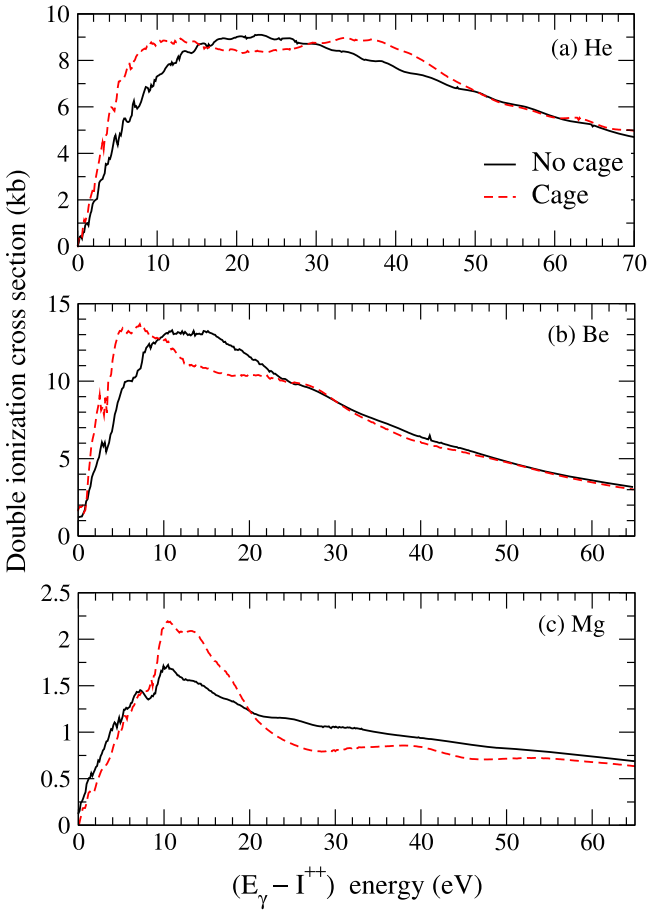

Figure 2. Double photoionization cross section for He, Be and Mg atoms as a function of excess photon energy. Comparison with cage atom and without cage.

figure 1 is to show the energy-dependent cross sections for total double photoionization of Be and Mg calculated using the implicit time propagator TDCC with core orthogonalization approach on a variable mesh method yield significantly better agreement; with a maximum difference of roughly 12%; with the RM method which is in good agreement with the experimental data. We note the earlier TDCC results for Be are about 20% lower in comparison to the RM data for photon energy range above 40 eV. In the case of Mg, on the other hand, the earlier TDCC results are lower but display greater discrepancy (with an average of ∼45%) as photon energy increases above 40 eV in comparison to the RM data.

The RMPS method is then extended to investigate photoionization cross sections for the endohedral Be and Mg. To examine the effects of the confining potential and the increasing size of the encapsulated atom, we also consider our previous RMPS result for He@C_{60} [22]. To enable a meaningful comparison of the three atoms, the double photoionization cross sections are plotted as a function of excess photon energy ($E_\gamma - I^{++}$), where E_γ is the photon energy and I^{++} is the double ionization threshold of the encapsulated atom. To elucidate the effect of C_{60} cage on the two-electron photoionization process, the cross sections are displayed along with the results for the three free atoms. Comparing the cage free and caged atoms, figure 2 clearly reveals the appearance of oscillatory structure in the total double photoionization cross sections of the confined atoms as one moves from He@C_{60} to Be@C_{60} and finally to Mg@C_{60}. Examining the profiles more carefully, one notices the resonances are separated by about 20 eV from each other and it is worth noting that in Mg@C_{60} the major peak is shifted by about 6 eV to higher energy with respect to Be@C_{60}. The shift on the energy scale is an effect of the effective potential [31], which indicates that in Be@C_{60} the potential is more attractive. As a result, the resonance profile is shifted to lower energy. This is a typical property of the metal atom; the valence electrons of Be atom are more bound than those of Mg due to the less effective screening in the former. Considering the fullerene potential to be static, it is not surprising to expect this property to be well retained also in the encapsulated compound.

Figure 3 shows the corresponding ratios of endofullerene cross sections to the cage free atoms. Looking at the trend

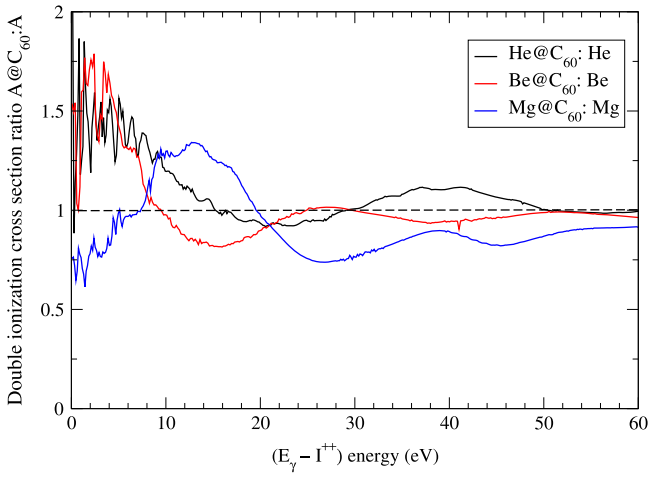

Figure 3. Ratio of double photoionization cross section of $A@C_{60}$ to A as a function of excess energy.

with different enclosed atoms in the fullerene, the confinement resonances appear to be sensitive to the size of the atoms enclosed in the C_{60} cage. First, we notice the ratios are shifted in phase as the the size of the enclosed atom increases (i.e., $r_{He} \sim 0.6$, $r_{Be} \sim 2.1$ and $r_{Mg} \sim 2.7$ a.u., where r_A is the radius of an atom in its ground state). Second, the ratios damp out with the growth of the photon energy and rapidly approach the asymptotic value of one. Third, in the case of $Mg@C_{60}$, there is a drop in the ratio near the double ionization threshold. This implies that the double ionization cross sections are suppressed for low ejected photoelectron energies. This allows us to conjecture, since the size of the central atom is larger; the valence electrons are more diffuse and closer to the fullerene shell; there is a greater chance that the presence of the Coulomb barrier of C_{60} is felt more strongly by the slower photoelectrons as they emit from the ground state of the enclosed Mg compared to the rest of the atoms in question. In another word, one may envisage, during the photoionization process the slow photoelectrons may feel a stronger confinement and hence causes the reduction of the double photoionization probability.

On the other hand, in our previous study of the double photoionization of helium confined in different fullerene cages, namely, C_{36}, C_{60} and C_{82} [32], we found the confinement resonances vary as we varied the cage cavity. This variation comes from the change in the positions of the constructive and destructive interference taking place between the reflected photoelectron waves from the fullerene boundary and the photoelectron waves emitted by the confined atoms. Interestingly, there we also found, in comparison to those of $He@C_{60}$ and $He@C_{82}$, the confinement resonances appeared to be damped for $He@C_{36}$. It seems a critical cage size may be necessary in order to induce confinement resonances in the double photoionization cross sections. This can be understood from the C_{36} was a strong enhancement of the single photoionization with excitation to n = 3 cross section, which physically would correspond to single photoionization with the other photoelectron captured to the C_{36} fullerene shell. Therefore, it seems as one makes the cage radius smaller one

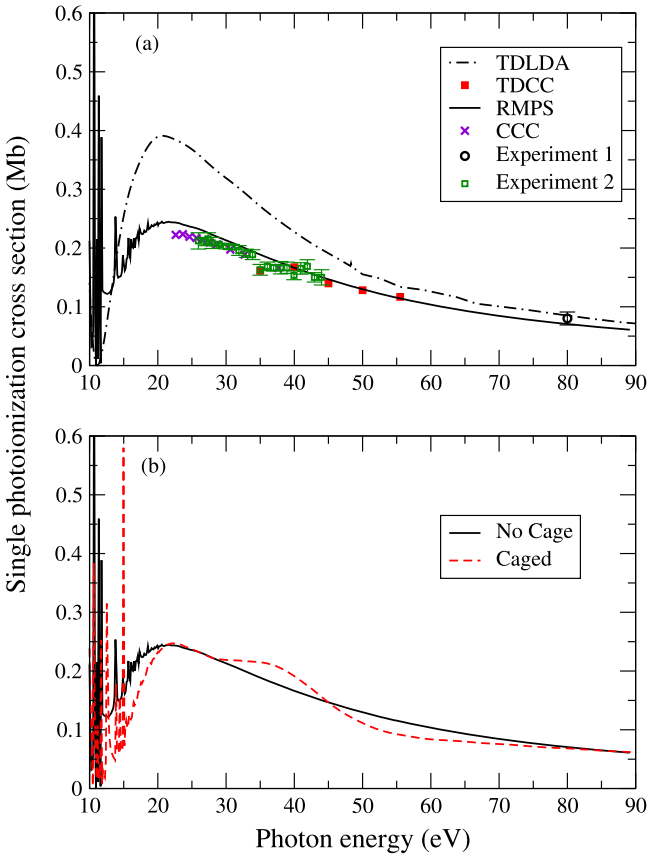

Figure 4. (a) Single photoionization cross section of Mg. Solid-line: present RMPS calculation, square: present TDCC calculation, dashed–dotted line: TDLDA calculation [39, 40] and ×: CCC calculation [36]. Experiment 1: data from [38] and experiment 2: data from from Wehlitz, Juranic and Lukic [37]. (b) Comparison with and without cage.

would enhance this process which in turn would reduce the flux going into the double photoionization channel.

The RMPS method allows one to calculate the cross sections not only for the single photon double photoionization, but also for the single ionization. In terms of the RMPS calculation, the total single photoionization can be obtained through the sum of the cross sections for photoionization to those final ionic sttaes that lie below the double ionisation threshold, as opposed to those above, which the summation would represent the double photoionization.

The RMPS results for the single ionization cross section for the caged and free Mg atoms are presented in figure 4. It is of great interest to compare the photoionization cross section for the caged and free Mg atoms, together with the experimental data available for the free Mg atoms [37, 38]. Besides, it also provides us another way to check the results of the present RMPS calculations. Shown along with the RMPS calculations in figure 4(a) are the photoionization cross section results obtained from other theoretical methods. Between 15 and 45 eV of photon energies, the results obtained using the RMPS method are considerably lower than the time-dependent local density approximation (TDLDA) method [39, 40], but are in good agreement with those from the TDCC and CCC calculations [36]. On the other hand, as

the photon energy increases, the RMPS and TDCC data practically overlap with each other with an exception that the TDLDA data remain slightly above the non-perturbative close-coupling results. Nonetheless, all theoretical data display good agreement with each other, as well as with the experimental measurement. The discrepancy between the TDLDA and the close-coupling calculations in the low energy region remains a puzzle. Figure 4(b) shows a comparison of the photoionization cross sections for the caged and free Mg atom. The presence of the confinement resonances in the case of $Mg@C_{60}$ is obvious.

4. Summary

In summary, we have sought to extend the RMPS method beyond the case of He to explore the double photoionization cross sections of $Be@C_{60}$ and $Mg@C_{60}$. Within the RMPS method, we employed a simple but well-tested square-well potential to model the C_{60} cage. We found the presence of confinement induced resonances for both $Be@C_{60}$ and $Mg@C_{60}$. To gain some understanding of effects of the confining potential and the increasing size of the atoms encapsulated in the fullerene cage, we compared the present photoionization results with our earlier study of $He@C_{60}$. Examining the resonance profile in the double photoionization cross sections for the the three endofullerene compounds, we found the separation between two resonant peaks in energy scale are relatively constant and consistent with a value of ~20 eV. We also observed, in comparison to $Be@C_{60}$, the major peak in $Mg@C_{60}$ is shifted by about 6 eV to higher energy, indicating in $Be@C_{60}$ the potential is more attractive. On the other hand, carefully looking at the confined-to-free atom double photoionization cross section ratios for endofullerene compounds, we noticed an interesting phase shift as one moves from $He@C_{60}$ to $Be@C_{60}$, to $Mg@C_{60}$. Furthermore, we observed in the case of $Mg@C_{60}$ the double ionization cross sections near the double ionization threshold. As a result, we conjectured the suppression is caused by the presence of the Coulomb barrier of C_{60} felt more strongly by the slower photoelectrons as they emit from the valence shell of Mg than the smaller atoms enclosed in the C_{60} cage.

Apart from the double photoionization process, we also examined the energy dependence of the single ionization cross section for $Mg@C_{60}$ compound and a free Mg atom. We compared our RMPS results for the free Mg atom with other theoretical and experimental data. It is found, between 15 and 30 eV of photon energies, the RMPS results are much lower than the TDLDA, however, they are in good agreement with the TDCC and CCC calculations. As the photon energy increases, all theoretical data agree very well with each other and together they are in good agreement with the experimental data. All told, with this work, we hope to motivate experimentalists and other theorists to undertake further investigations on the endohedral alkaline-Earth metals.

Acknowledgments

We thank Himadri Chakraborty of Northwest Missouri State University for sending us the TDLDA data. TWG was supported in part by NASA (NNX11AF32G). This work was supported in part by grants from the US Department of Energy and the US National Science Foundation. Computational work was carried out at the National Energy Research Scientific Computing Center in Oakland, California, and the National Institute for Computational Sciences in Knoxville, Tennessee.

References

[1] Tang J Z and Shimamura I 1995 *Phys. Rev.* A **52** R3413
[2] Tang J Z and Burgdöfer J 1997 *J. Phys. B: At. Mol. Opt. Phys.* **30** L523
[3] Kheifets A S and Bray I 1996 *Phys. Rev.* A **54** R995
[4] Meyer K W, Greene C H and Esry B D 1997 *Phys. Rev. Lett.* **78** 4902
[5] Meyer K W, Bohn J L, Greene C H and Esry B D 1997 *J. Phys. B: At. Mol. Opt. Phys.* **30** L641
[6] Gorczyca T W and Badnell N R 1997 *J. Phys. B: At. Mol. Opt. Phys.* **30** 3897
[7] Pindzola M S and Robicheaux F 1998 *Phys. Rev.* A **57** 318
[8] Pindzola M S and Robicheaux F 1998 *Phys. Rev.* A **58** 779
[9] Colgan J and Pindzola M S 2002 *Phys. Rev.* A **65** 032729
[10] Colgan J and Pindzola M S 2003 *Phys. Rev.* A **67** 012711
[11] Levin J C, Armen G B and Sellin I A 1996 *Phys. Rev. Lett.* **76** 1220
[12] Dorner R *et al* 1996 *Phys. Rev. Lett.* **76** 2654
[13] Samson J A R, Stolte W C, He Z-X, Cutler J N, Lu Y and Bartlett R J 2003 *Phys. Rev.* A **57** 1906
[14] Dolmatov V K 2009 *Advances in Quantum Chemistry* (*Theory of Confined Quantum Systems: Part Two* vol 58) ed J R Sabin and E Brändas (New York: Academic) pp 13–68
[15] Kilcoyne A L D *et al* 2010 *Phys. Rev. Lett.* **105** 213001
[16] Müller A, Schippers A, Habibi H, Esteves D, Wang J C, Phaneuf R A, Kilcoyne A L D, Aguilar A and Dunsch L 2008 *Phys. Rev. Lett.* **101** 133001
[17] Amusia M Y, Liverts E Z and Mandelzweig V B 2006 *Phys. Rev.* A **74** 042712
[18] Ludlow J A, Lee T-G and Pindzola M S 2010 *Phys. Rev.* A **81** 023407
[19] Ludlow J A, Lee T-G and Pindzola M S 2010 *J. Phys. B: At. Mol. Opt. Phys.* **43** 235202
[20] Gorczyca T W, Hasoˇglu M F and Manson S T 2012 *Phys. Rev.* A **86** 033204
[21] Hasooˇlu M F, Zhou H-L, Gorczyca T W and Manson S T 2013 *Phys. Rev.* A **87** 013409
[22] Gorczyca T W, Lee T-G and Pindzola M S 2013 *J. Phys. B: At. Mol. Opt. Phys.* **46** 195201
[23] Griffin D C, Pindzola M S, Ballance C P and Colgan J 2009 *Phys. Rev.* A **79** 023417
[24] Broclawik E and Eilmes A 1998 *J. Chem. Phys.* **108** 3498
[25] Xu Y B, Tan M Q and Becker U 1996 *Phys. Rev. Lett.* A **76** 3538
[26] Dolmatov V K and Manson S T 2006 *Phys. Rev.* A **73** 013201
[27] Lee T-G, Ludlow J A and Pindzola M S 2013 *Phys. Rev.* A **87** 015401
[28] Badnell N R 2011 *Comput. Phys. Commun.* **182** 1528
[29] http://physics.nist.gov/PhysRefData/contentes-atomic.html
[30] Pindzola M S, Ballance C P, Abdel-Naby S A, Robicheaux F, Armstrong G S J and Colgan J 2013 *J. Phys. B: At. Mol. Opt. Phys.* **46** 035201

[31] Stener M, Lisini A and Decleva P 1995 *Int. J. Quantum Chem.* **53** 229
[32] Lee T-G, Ludlow J A and Pindzola M S 2012 *J. Phys. B: At. Mol. Opt. Phys.* **45** 135202
[33] Colgan J and Pindzola M S 2002 *Phys. Rev.* A **65** 022709
[34] Kheifets A S and Bray I 2001 *Phys. Rev. A* **65** 012710
[35] Wehlitz R, Lukic D and Bluett J B 2005 *Phys. Rev.* A **71** 012707
[36] Kheifets A S and Bray I 2007 *Phys. Rev.* A **75** 042703
[37] Wehlitz R, Juranic P N and Lukic D 2008 *Phys. Rev.* A **78** 033428
[38] Hausmann A, Kammerling B, Kossmann H and Schmidt V 1988 *Phys. Rev. Lett.* **61** 2669
[39] Chakraborty H S, Madjet M E, Rost J-M and Manson S T 2008 *Phys. Rev.* A **78** 013201
[40] Chakraborty H S 2015 private communication